α-decays of neutron-deficient americium isotopes

M. Sakama*
Department of Radiologic Science and Engineering, School of Health Sciences, The University of Tokushima, Tokushima 770-8509, Japan

M. Asai, K. Tsukada, S. Ichikawa, I. Nishinaka, and Y. Nagame
Advanced Science Research Center, Japan Atomic Energy Research Institute, Tokai, Ibaraki 319-1195, Japan

H. Haba
Cyclotron Center, The Institute of Physical and Chemical Research (RIKEN), Wako, Saitama 351-0198, Japan

S. Goto
Department of Chemistry, Niigata University, Niigata 950-2181, Japan

M. Shibata
Radioisotope Research Center, Nagoya University, Nagoya 464-8602, Japan

K. Kawade
Department of Energy Engineering and Science, Nagoya University, Nagoya 464-8603, Japan

Y. Kojima
Graduate school of Engineering, Hiroshima University, Higashi-Hiroshima 739-8527, Japan

Y. Oura, M. Ebihara, and H. Nakahara
Department of Chemistry, Tokyo Metropolitan University, Hachioji, Tokyo 192-0397, Japan
(Received 28 September 2003; published 23 January 2004)

Neutron-deficient americium isotopes ^{233,234,235,236}Am were produced in the bombardment of multiple thin targets of ^{233}U and ^{235}U with 7.6–10.5 MeV/nucleon ^{6}Li ions. The reaction products were effectively mass-separated using the on-line isotope separator (JAERI-ISOL) coupled to a helium gas-jet transport system. For the first time, the α transition of ^{235}Am was observed, and some improved α-decay data for ^{233,234,236}Am and ^{229}Np (α-decay daughter of ^{233}Am) were accumulated. The α-particle energies of ^{233}Am and ^{235}Am were determined to be 6780 ± 17 keV and 6457 ± 14 keV and their half-lives were 3.2 ± 0.8 min and 10.3 ± 0.6 min, respectively. Measured α-decay branching ratios of ^{235}Am and ^{229}Np were $(4.0\pm0.5)\times10^{-3}$ and 0.68 ± 0.11, respectively, while the lower limit for α-decay of ^{233}Am was deduced to be 3×10^{-2}. Hindrance factors and probable assignments of the levels involved in those α transitions are discussed.

DOI: 10.1103/PhysRevC.69.014308 PACS number(s): 23.60.+e, 27.90.+b

I. INTRODUCTION

Nuclear decay properties of neutron-deficient actinides, including americium isotopes, provide us invaluable information. In particular, the α-particle energies obtained are useful for precise determination of nuclear mass, which is one of the most essential quantities for defining nuclear decay properties, shell stability, and fusion probabilities. In addition, α-decay half-lives and the fine structure of α-particle spectra bring us information on the nuclear structure of daughter nuclei close to the proton drip line. However, since the neutron-deficient actinides decay predominantly by electron capture (EC), and their α-decay branching ratios are extremely small, only a few investigations of neutron-deficient americium isotopes have been conducted in the last 13 years. Examples are the EC-delayed fission of ^{232}Am and ^{234}Am by Hall *et al.* [1–3] and the EC decay of ^{235}Am by Guo *et al.* [4]. In particular, regarding the α-decays of the americium isotopes with half-lives shorter than 1 h, only a limited number of α-decay data are currently available in the literature. Recently, we have succeeded in observing EC and α-decays of ^{236}Am [5] and ^{233}Am [6], respectively, using the JAERI on-line isotope separator coupled to the helium gas-jet transport system [7]. In this paper, we present new and improved data on the α-decay of ^{233}Am, ^{234}Am, ^{235}Am, ^{236}Am, and ^{229}Np (α-decay daughter of ^{233}Am). These results are then discussed in the general trend of α-decay properties. Some of the present data on the EC decay of ^{236}Am and on the identification of ^{233}Am have been partly described in our previous papers [5,6].

II. EXPERIMENT

Experiments were performed using the JAERI on-line isotope separator (JAERI-ISOL) coupled to the helium gas-jet

*Corresponding author. Electronic address: sakama@medsci.tokushima-u.ac.jp

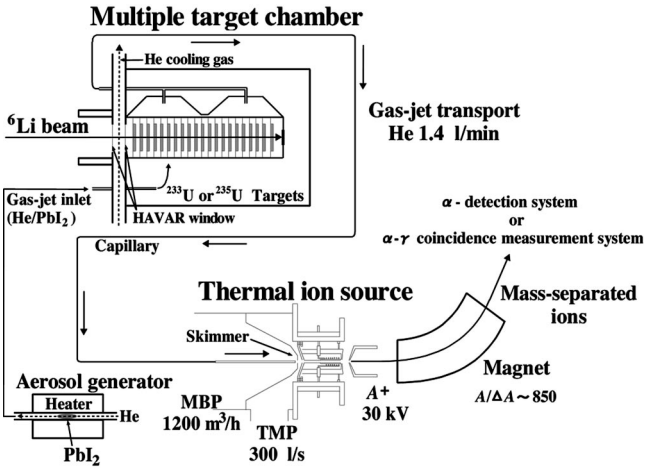

FIG. 1. Schematic diagram of the gas-jet coupled JAERI-ISOL. The gas-jet transport system consists of the aerosol generator, the multiple-target chamber, and the vacuum system which consists of a mechanical booster pump (MBP) and a turbomolecular pump (TMP) for the differential pumping.

transport system. A schematic view of the experimental setup is shown in Fig. 1. Neutron-deficient americium isotopes were produced via the reactions of ^{233}U(^{6}Li, 6n)^{233}Am, ^{233}U(^{6}Li, 5n)^{234}Am, ^{233}U(^{6}Li, 4n)^{235}Am, and ^{235}U(^{6}Li, 5n)^{236}Am. A stack of 21 ^{233}U (or ^{235}U) targets set in a multiple-target chamber with 5 mm spacings was bombarded with ^{6}Li beam intensities ranging from 250 to 340 particle-nA, delivered from the JAERI tandem accelerator. Each target was prepared by electrodeposition of $UO_2(NO_3)_2$ in 2-propanol onto a 0.9 mg/cm^2 thick aluminum backing foil. Target thicknesses were in the range of 50–130 μg/cm^2 for ^{233}U and 160–420 μg/cm^2 for ^{235}U. Incident beam energies were 63.0 MeV for the production of ^{233}Am, 45.5 MeV for ^{235}Am, and 51.0 MeV for ^{234}Am and ^{236}Am. The ^{6}Li beam passed through two HAVAR vacuum windows (4.6 mg/cm^2) and helium cooling gas (0.1 mg/cm^2), with its energy finally reduced to 52–60 MeV on the targets for the 63.0 MeV incident beam energy, 34–42 MeV for 45.5 MeV, and 39–48 MeV for 51.0 MeV. Reaction products recoiling out of the targets were stopped by He gas (94 kPa) loaded with PbI_2 aerosol clusters. The products attached to the clusters were continuously swept out of the target chamber with a 1.4 l/min He gas flow and transported to a thermal ion source of the ISOL through a Teflon capillary (1.5 mm in

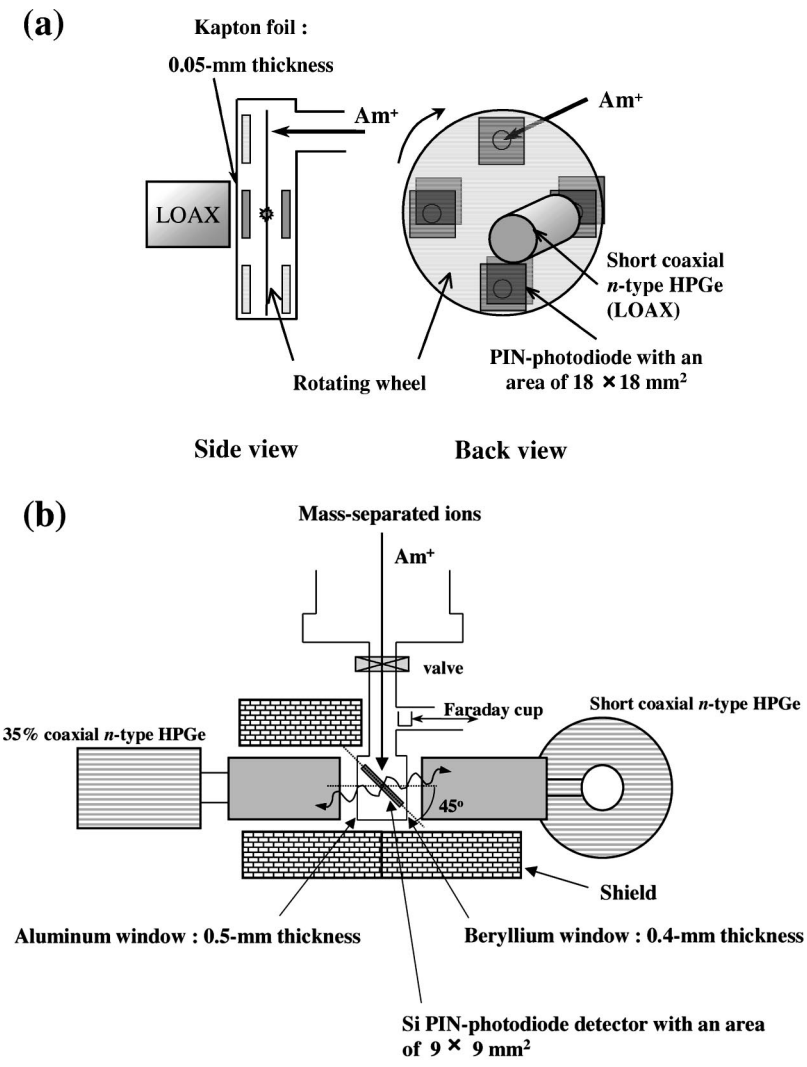

FIG. 2. Setup of the detection systems: (a) the rotating wheel system for α spectrometry and (b) the α-γ and γ-γ coincidence measurement system.

diameter and 8 m length). Atoms ionized in the ion source were accelerated with 30 kV and mass separated with a resolution of $A/\Delta A \sim 850$ at the mass number $A=208$ [7]. The overall efficiency including the gas-jet transport and the ionization of americium atoms was measured to be $(0.3\pm0.1)\%$ through the observation of ^{237}Am produced in the ^{235}U(^{6}Li, $4n$) reaction [8].

Figure 2(a) shows a schematic drawing of the rotating wheel α-detection system. The mass-separated ions were implanted into 10 μg/cm^2 thick polyvinylchloride-acetate copolymer foils placed around the periphery of the rotating wheel. The wheel periodically rotated by 90° with appropriate intervals, which carried the implanted sources to three consecutive detector stations. Each detector station was equipped with two Si detectors (HAMAMATSU PIN-photodiode S3204-09, 18×18 mm^2 active area [9,10]) that surrounded the source on the wheel to measure α particles with an efficiency of 85%. Another Si detector was placed at the implantation station in the forward direction of the ion implantation. In order to determine α/EC branching ratios, characteristic x rays following the EC decay were measured at the first detector station through a window made of Kapton foil (0.05 mm in thickness) using a short coaxial Ge detector (ORTEC LOAX^{TM}, $51\phi\times21$ mm thickness of Ge, full width at half maximum of 0.66 keV at 122 keV γ ray). The energy calibration of the Si detectors was performed using mass-separated ^{221}Fr($E_\alpha=6341$ keV) and its α-decay daughters ^{217}At(7067 keV) and ^{213}Po(8376 keV). The ^{221}Fr nuclei recoiling out of the ^{225}Ac α source were transported to the ion source of the ISOL by a gas-jet stream, and the mass-separated ions were implanted into the same foils that were used in the on-line experiments for Am isotopes. The α-particle energy resolution was about 45 keV.

For ^{235}Am, α-γ and γ-γ coincidence measurements were performed using another experimental setup shown in Fig. 2(b). The mass-separated ions were implanted into the Si detector (HAMAMATSU PIN-photodiode S3590-06, 9×9 mm^2 active area [9,10]) which was tilted by 45° with respect to the ion beam axis. The detection chamber containing the Si detector had an aluminum window of 0.5 mm thickness and a beryllium one of 0.4 mm thickness toward the two endcaps of two Ge detectors placed on both sides of the Si detector; one was a short coaxial Ge detector placed on the front side of the Si detector to detect low-energy photons down to $\sim$10 keV and the other was a 35% n-type Ge detector (ORTEC GAMMA-X^{TM}) on the opposite side. The detectors were shielded with 100 mm thick lead bricks and 5 mm thick copper inner plates. α- and x/γ-ray singles and α-γ and γ-γ coincidence data were recorded event by event together with time information.

III. RESULTS

A. ^{236}Am

The sum of α-particle spectra measured with the seven Si detectors for the mass-236 fraction accumulated during a period of 270 s$\times$380 cycles is shown in Fig. 3(a), and the x/γ-ray spectrum associated with the EC decay of ^{236}Am during the same experimental run is shown in Fig. 4(a). The

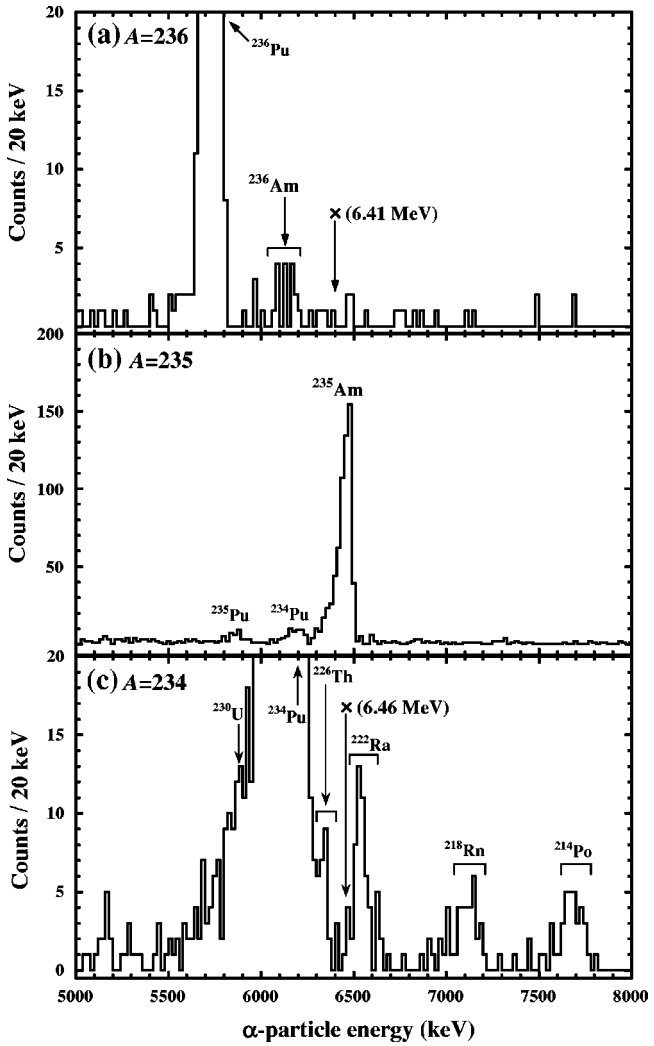

FIG. 3. Sum of α-particle spectra in the mass fraction of A= (a) 236, (b) 235, and (c) 234. Crosses shown in (a) and (c) indicate the 6.41 MeV α group of ^{236}Am and 6.46 MeV one of ^{234}Am reported by Hall *et al.*, respectively [1,3].

α-decay of ^{236}Am was reported by Hall *et al.* [3], who observed a 6.41 MeV α group and its α/EC branching ratio of $(4.2\pm0.6)\times10^{-4}$. However, no 6.41 MeV α group was observed in the present experiment [see Fig. 3(a)], and the upper limit of the α branching around 6.41 MeV was deduced to be 2×10^{-5}. Instead, a very weak α group around 6150 keV is observed in the spectrum. The decay curve of this α group gives a half-life of 3.1 ± 1.3 min as shown in Fig. 5, which is consistent with that of 3.6 ± 0.1 min for the decay of the Pu $K_{\alpha1}$ x ray associated with the EC decay of ^{236}Am in the same experimental run. In addition, from the γ-γ coincidence measurement data in Ref. [11], it has been found that there are two EC-decaying states (^{236}Am^g and ^{236}Am^m) in ^{236}Am and their half-life values of 3.6 ± 0.2 min for ^{236}Am^g and 2.9 ± 0.2 min for ^{236}Am^m are very close to each other. Those half-lives are also in agreement with that of the present 6150 keV α group. Thus, we conclude that the observed 6150 keV α group is attributable to the α-decay of ^{236}Am. [In the γ-γ coincidence measurement, we know that the yields of mass-separated ^{236}Am^g and ^{236}Am^m are ap-

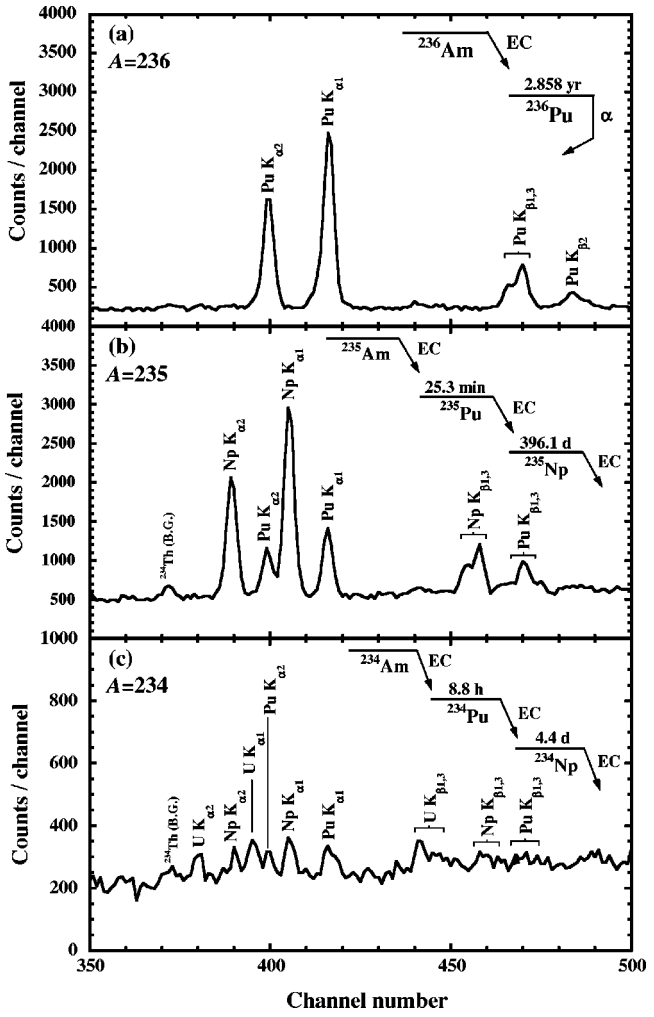

FIG. 4. x/γ-ray spectra in the mass fraction of A= (a) 236, (b) 235, and (c) 234. Each inset shows the EC-decay chains from ^{236}Am, ^{235}Am, and ^{234}Am.

proximately equal in the ^{235}U(^{6}Li, 5n) reaction, and their contributions to the Pu K x-ray intensity are also expected to be about the same. However no clear assignment of the α group to either one of those isomers could be made in the present experiment.] The α branching of $I_\alpha = (4.0 \pm 1.0) \times 10^{-5}$ was derived from the ratio between the observed 6150 keV α intensity and that of the Pu K x ray. The production cross section σ_{expt} of ^{236}Am^{g+m} at the ^{6}Li beam energy of 39–48 MeV was determined to be 125 ± 46 μb by use of the detection efficiency for Pu K x rays and the overall efficiency of (0.3 ± 0.1)% for americium atoms in the ISOL system.

B. ^{235}Am

The sum of measured α-particle spectra for the mass-235 fraction accumulated during 900 s $\times$ 360 cycles is shown in Fig. 3(b). The strong α line with the energy of 6457 ± 14 keV is unequivocally observed. In the x/γ-ray spectrum as shown in Fig. 4(b), Pu and Np K x rays associated with the EC decays of $^{235}\text{Am} \xrightarrow{\text{EC}} {}^{235}\text{Pu} \xrightarrow{\text{EC}} {}^{235}\text{Np}$ were clearly observed. Figure 6 shows decay curves of the 6457 keV α line and Pu K x rays. The deduced half-lives of 10.7 ± 0.7 min for the 6457 keV α line and 9.5 ± 1.2 min for the Pu $K_{\alpha 1}$ x ray are in good agreement within the experimental errors as shown in Fig. 6, indicating that the 6457 keV α line is attributable to the α-decay of ^{235}Am. We, in this paper, reanalyzed the EC-decay data [12] of ^{235}Am produced in the ^{235}U(^{6}Li, 6n)^{235}Am reaction and obtained a half-life of 9.0 ± 1.5 min. Taking a weighted average of these values, it was found that the total half-life of ^{235}Am obtained from the α- and EC-decay data was determined to be 10.3 ± 0.6 min which is marginally consistent with the literature value of 15 ± 5 min by Guo *et al.* [4]. The α branching of $I_\alpha = (4.0 \pm 0.5) \times 10^{-3}$ was for the first time derived from the

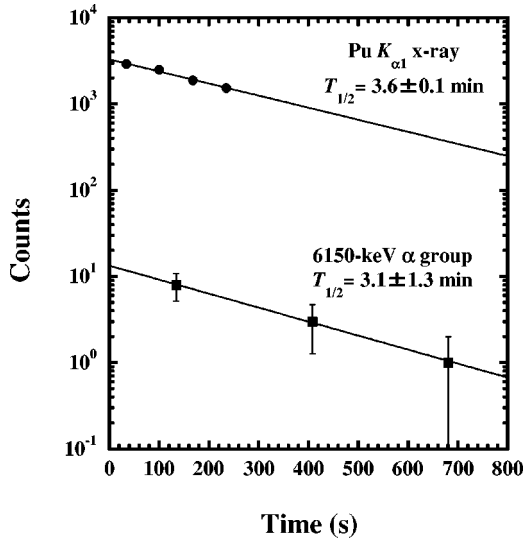

FIG. 5. Decay curves of the 6150 keV α group emitted from the α-decay of ^{236}Am and the Pu $K_{\alpha 1}$ x ray associated with the EC decay of ^{236}Am.

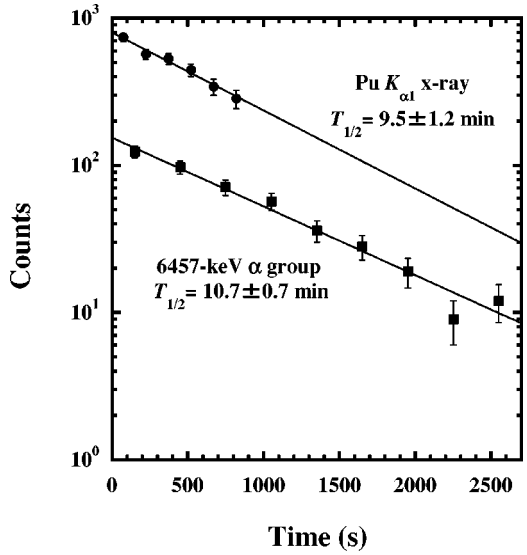

FIG. 6. Decay curves of the 6457 keV α group emitted from the α-decay of ^{235}Am and the Pu $K_{\alpha 1}$ x ray associated with the EC decay of ^{235}Am.

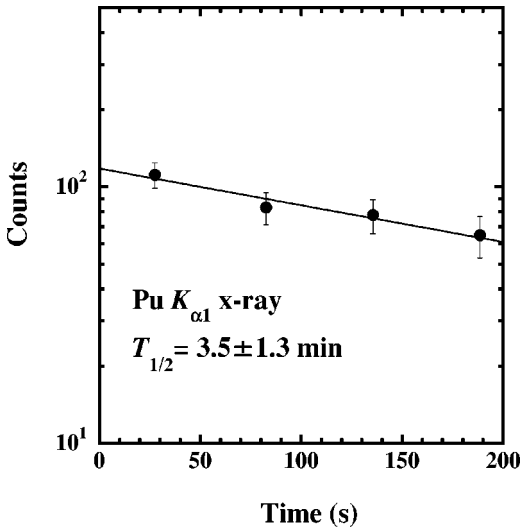

FIG. 7. Decay curve of the Pu $K_{\alpha 1}$ x ray associated with the EC decay of ^{234}Am.

ratio between the observed α- and Pu K x-ray intensities.

In the α-particle spectrum shown in Fig. 3(b), the two weak α lines around 5800 keV and 6200 keV arising from the α-decays of ^{235}Pu and ^{234}Pu, respectively, are also barely discernible. In the assignment of ^{235}Pu, we know that ^{235}Pu decays very weakly via α-particle emission with $I_\alpha = (3.0 \pm 0.6) \times 10^{-5}$ and $E_\alpha = 5.85 \pm 0.02$ MeV [13]. One notices that the ratio of the intensity of the Np $K_{\alpha 1}$ x ray to that of the Pu $K_{\alpha 1}$ x ray is $\sim$2.9 [see Fig. 4(b)], which is much larger than the expected value of 0.6 on the basis of the growth and decay of ^{235}Pu associated with the EC decay of ^{235}Am. Thus, it can be stated that the ^{235}Pu is directly produced via the ^{233}U(^{6}Li, $p3n$)^{235}Pu reaction as well as through the EC decay of ^{235}Pu. In the assignment of ^{234}Pu, since ^{234}Pu decays with $I_\alpha = 4.8\%$ and $E_\alpha = 6202$ keV [14], and the mass resolution performance of the ISOL allows a slight inclusion of the $A = 234$ nuclides, it is not surprising that the observed α particles around 6200 keV originated from the α-decay of ^{234}Pu.

In the α-γ coincidence measurement, although the sum of 230 α particles was detected at 6457 keV, no α-γ coincidence event was observed. This result suggests that the level fed by the 6457 keV α transition is either the ground state of ^{231}Np or a low lying level that decays via internal conversion. The production cross section of the ^{233}U(^{6}Li, $4n$)^{235}Am reaction at the ^{6}Li beam energy of 34–42 MeV was determined to be 31 ± 12 μb, that is, about six times larger than 5 ± 2 μb of the ^{235}U(^{6}Li, $6n$)^{235}Am reaction reported in Ref. [12].

C. ^{234}Am

Figure 4(c) shows the x/γ-ray spectrum observed in the mass-234 fraction during the detection period of 210 s $\times$ 550 cycles. Pu, Np, and U K x rays associated with the EC decays of ^{234}Am, ^{234}Pu, and ^{234}Np, respectively, are clearly seen in the spectrum. The observed peak intensities of the Np

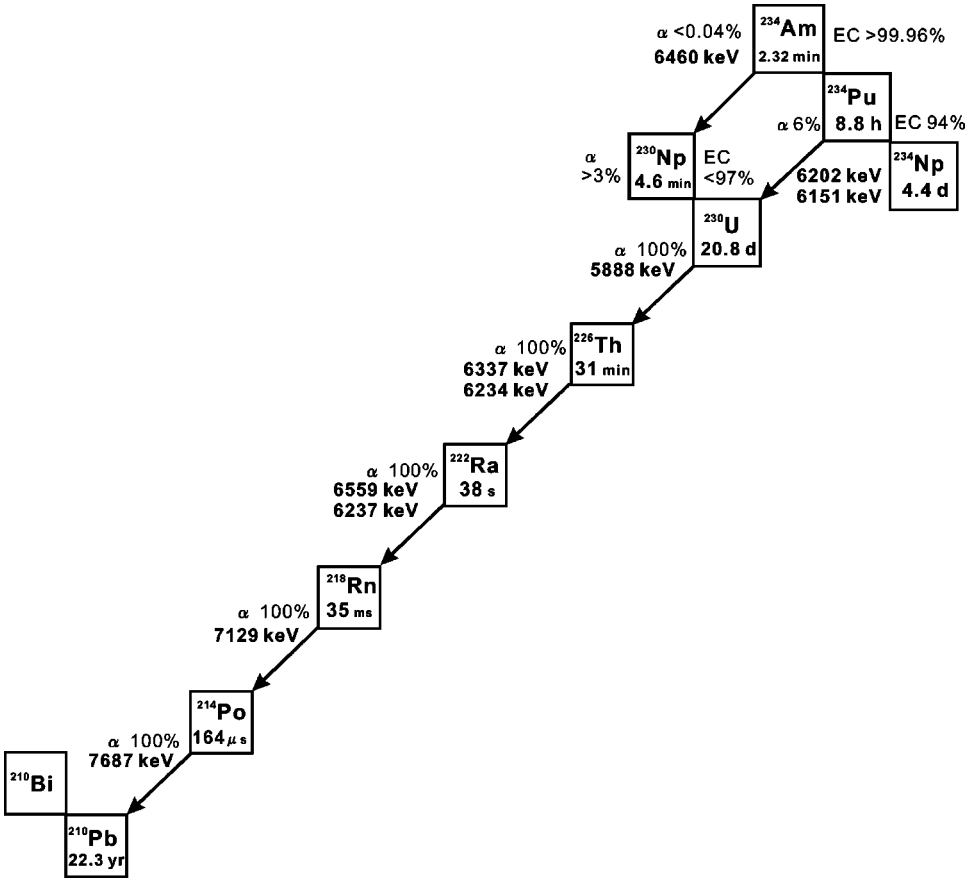

FIG. 8. α- and EC-decay chains originating from ^{234}Am. Data from Ref. [14].

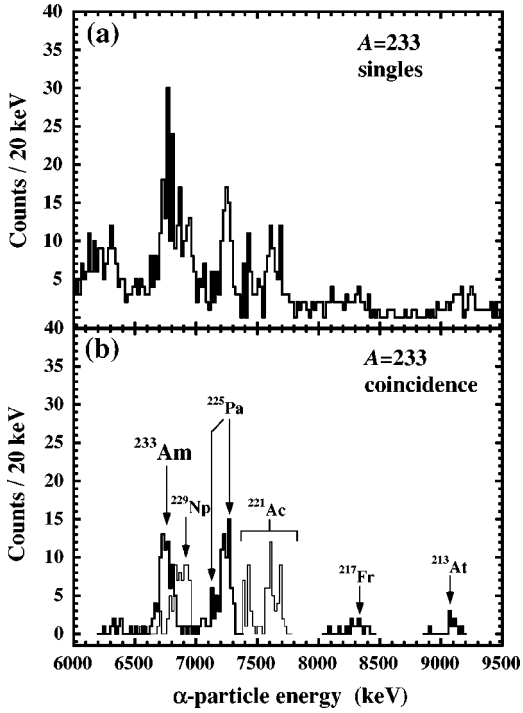

FIG. 9. (a) Singles α-particle spectrum observed in the mass fraction $A=233$. (b) Coincidence α-particle spectrum constructed from the measured α-α correlation events associated with the α-decay of ^{233}Am.

and U K x rays are found larger than those of the Pu K x rays expected from the EC decay of ^{234}Am. The excess production of ^{234}Pu and ^{234}Np may be attributable to reactions such as ^{233}U(^{6}Li, $p4n$) and ^{233}U(^{6}Li, αn). The half-life of 3.5 ± 1.3 min derived from the decay curve of the Pu $K_{\alpha1}$ x ray as shown in Fig. 7 is consistent with that of 2.32 ± 0.08 min reported by Hall *et al.* [1] from the analysis of the decay curve of the EC-delayed fission events of ^{234}Am.

For the α-decay of ^{234}Am, the observed spectrum is shown in Fig. 3(c) in which a series of α lines associated with the α-decay chain of

$$^{234}\mathrm{Pu}\xrightarrow{\alpha}{}^{230}\mathrm{U}\xrightarrow{\alpha}{}^{226}\mathrm{Th}\xrightarrow{\alpha}{}^{222}\mathrm{Ra}\xrightarrow{\alpha}{}^{218}\mathrm{Rn}\xrightarrow{\alpha}{}^{214}\mathrm{Po}\xrightarrow{\alpha}{}^{210}\mathrm{Pb}$$

(see Fig. 8) are detected. The 6.46 MeV α group for ^{234}Am with α branching of $(3.9\pm1.2)\times10^{-4}$ was reported by Hall *et al.* [1]; however, no such α particles were observed within an upper limit of $I_\alpha<4\times10^{-4}$. The production cross section of ^{234}Am at the ^{6}Li beam energy of 39–48 MeV was deduced to be 9 ± 5 μb from the intensity of the observed Pu $K_{\alpha1}$ x ray.

D. ^{233}Am

Identification of the new nuclide ^{233}Am via the α-α correlation analysis has been described in our previous paper

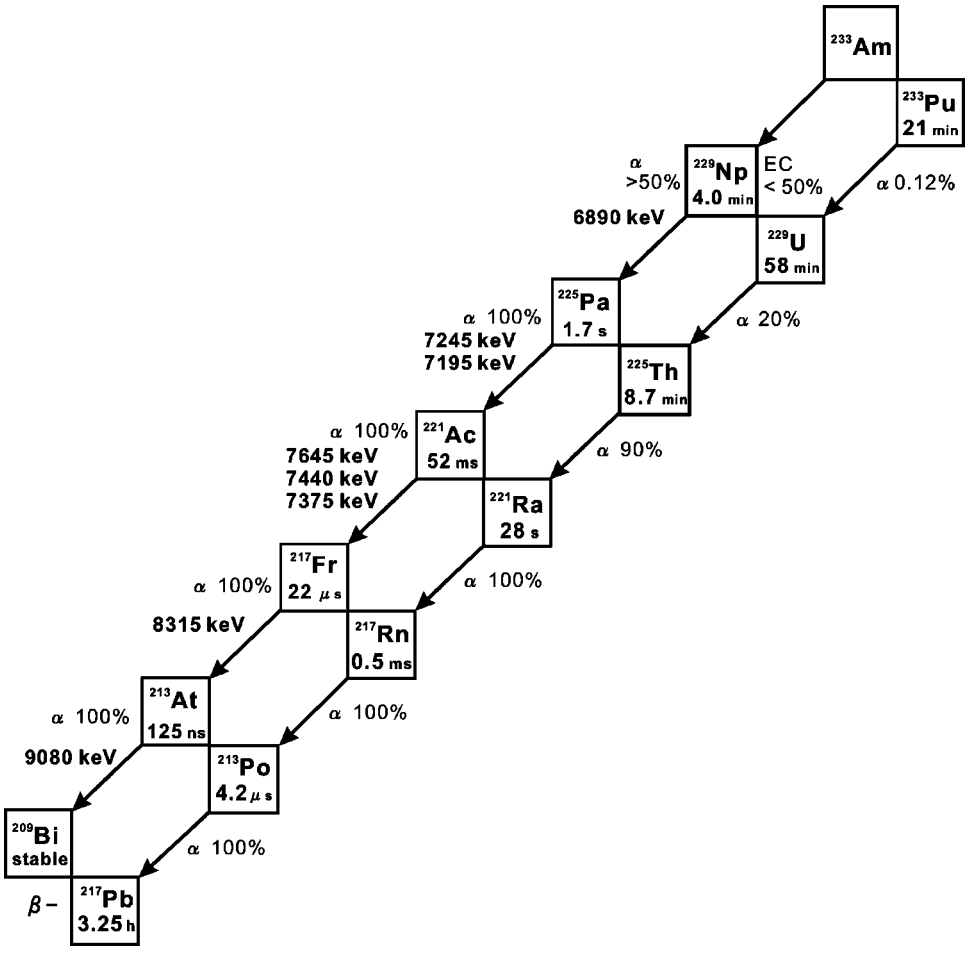

FIG. 10. α-decay chains originating from ^{233}Am. Data from Ref. [14].

TABLE I. α-decay properties of the neutron-deficient Am and Np isotopes.

		This work				Literature		
Nuclide	Reaction	$\sigma_{expt}(\mu b)$[a]	$T_{1/2}$ (min)	E_α (keV)	I_α	$T_{1/2}$ (min)	E_α (keV)	I_α
$^{236}Am^{g+m}$	$^{235}U(^6Li, 5n)$	125±46	3.6±0.1	6150	$(4.0\pm0.1)\times10^{-5}$	4.4±0.8 [5]	6410 [3]	$(4.2\pm0.6)\times10^{-4}$ [3]
^{235}Am	$^{233}U(^6Li, 4n)$	31±12	10.3±0.6	6457±14	$(4.0\pm0.5)\times10^{-3}$	15±5 [4]		
^{234}Am	$^{233}U(^6Li, 5n)$	9±5	3.5±1.3	Not observed	$<4\times10^{-4}$	2.32±0.08 [1]	6460 [1]	$(3.9\pm1.2)\times10^{-4}$ [1]
^{233}Am	$^{233}U(^6Li, 6n)$	<0.9	3.2±0.8	6780±17	$>3\times10^{-2}$			
^{229}Np	α-decay daughter of ^{233}Am		4.0±0.4	6893±23	0.68±0.11	4.0±0.2 [15]	6890±20 [15]	>0.50 [15]

[a]The production cross sections are evaluated using the overall efficiency of (0.3±0.1)% for americium atoms in the present experiments.

[6]. In the present paper, we briefly summarize α/EC-decay properties of ^{233}Am and ^{229}Np. Figures 9(a) and 9(b) show the singles and the delayed-coincident α-particle spectra observed in the mass-233 fraction, respectively. Since the α-decay of ^{229}Np is followed by four successive α-decays with short half-lives,

$$^{225}\mathrm{Pa}(1.7\ \mathrm{s})\xrightarrow{\alpha}{}^{221}\mathrm{Ac}(52\ \mathrm{ms})\xrightarrow{\alpha}{}^{217}\mathrm{Fr}(22\ \mu\mathrm{s})\xrightarrow{\alpha}{}^{213}\mathrm{At}(125\ \mathrm{ns})$$

as shown in Fig. 10, the α-α correlations among these five nuclei are unambiguously identified. In the present measurement, 99 α-α correlation events following the α-decay of ^{229}Np were observed in the mass-233 fraction. The α-particle energies of ^{233}Am and ^{229}Np were determined to be 6780±17 keV and 6893±23 keV, respectively, using the maximum-likelihood method [6]. The half-life of ^{233}Am was 3.2±0.8 min from the decay curve of 6780 keV α particles. In addition, from the time intervals between the α-decays of ^{233}Am and ^{229}Np, the half-life of ^{229}Np was evaluated to be 4.0±0.4 min. This value and the α-particle energy mentioned above agree well with the literature values of 4.0±0.2 min and 6890±20 keV reported by Hahn *et al.* [15]. For ^{229}Np, the α branching I_α of 0.68±0.11 was derived from the ratio between the measured α-α correlation events following the α-decay of ^{229}Np and those following the α-decay of ^{225}Th, which was accumulated from the α-decay of ^{229}U after the EC decay of ^{229}Np. The present α branching I_α is consistent with a value >0.50 reported by Hahn *et al.* [15]. Figure 11 shows the x/γ-ray spectrum in the mass-233 fraction that was measured using the tape transport detection system. No Pu $K_{\alpha1}$ x ray originating from the EC decay of ^{233}Am was observed in the present measurement, while U *K* x rays due to the EC decay of Np were detected. Considering the detection efficiency and the reaction system, it is likely that the ^{233}Np is produced via the nuclear transfer reaction and the observed U *K* x rays mostly originated from the EC decay of ^{233}Np. Based on the detection efficiencies of the α particles and Pu $K_{\alpha1}$ x ray, the α branching I_α of ^{233}Am was evaluated to be larger than 3.0×10^{-2}. Using the α branching I_α, the production cross section of ^{233}Am at the ^{6}Li beam energy of 52–60 MeV was deduced to be <0.9 μb as an upper limit.

Table I summarizes the α-decay properties of the neutron-deficient Am and Np isotopes, together with the literature data [1,3–5,15] and also their production cross sections.

IV. DISCUSSION

In general, a hindrance factor *F* is often used for understanding the nature of an α transition. Various empirical and theoretical formulas to derive the hindrance factor *F* from the relationship between the α-decay partial half-life and the α-transition energy have been presented in detail for even-even nuclides, for example, by Taagepera and Nurmia [16], Viola and Seaborg [17], Buck *et al.* [18], Hatsukawa *et al.* [19], and Preston [20]. In this paper, in order to evaluate the hindrance factors for the α-decays of neutron-deficient Am and Np nuclides, we have used a semiempirical formula for even-even nuclides given by Rasmussen [21], as we now discuss.

Figure 12 shows α-decay partial half-lives T_α for the ground-to-ground transitions in even-even nuclides of U, Pu, Cm, and Cf with $A=228-250$ as a function of the α-transition energy E_α^*. The data observed in the present work are plotted by open symbols for ^{235}Am, ^{236}Am, and ^{229}Np and by a vertical line showing error bars for α branching I_α ranging from 3.0×10^{-2} to 1.0 for ^{233}Am. The curves are drawn through favored transitions according to the following semiempirical function that shows the relationship between α-decay partial half-life T_α (s) and α-transition energy E_α^* (keV) in even-even nuclides (U, Pu, Cm, and Cf),

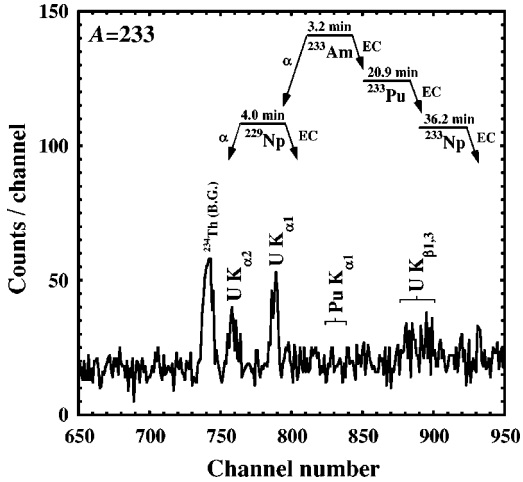

FIG. 11. x/γ-ray spectrum at the mass-233 fraction. The inset shows the α- and EC-decay chains from ^{233}Am. The observed U *K* x rays originate from the EC decay of ^{233}Np which was directly produced via the reaction of ^{233}U+^{6}Li.

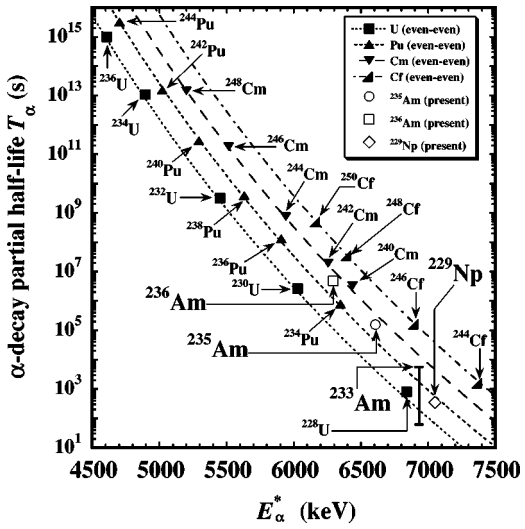

FIG. 12. α-decay partial half-lives for even-even uranium, plutonium, curium, and californium nuclei with $A=228-250$ plotted as a function of the α-transition energy. The dotted curve is expressed as the semiempirical function fitted for even-even $^{228-236}$U data points, the dashed one is for even-even $^{234-244}$Pu, the long dashed one for even-even $^{240-248}$Cm, and the dash-dotted one for even-even $^{244-250}$Cf. The present data are plotted by open symbols for ^{235}Am, ^{236}Am, and ^{229}Np and by a vertical line showing the error bar as the α branching of $3.0\times10^{-2}<I_\alpha<1.0$ for ^{233}Am.

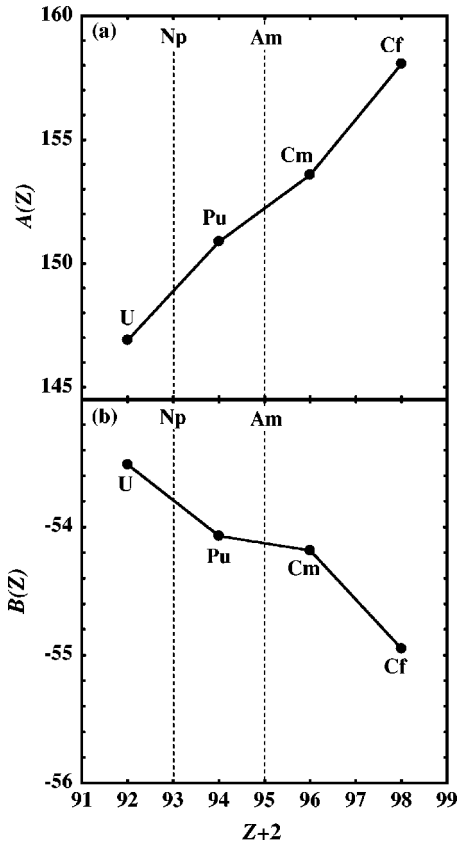

FIG. 13. Correlations between semiempirical $A(Z)$ (upper) and $B(Z)$ (lower) constants and $(Z+2)$ of the even-even nuclei (see text).

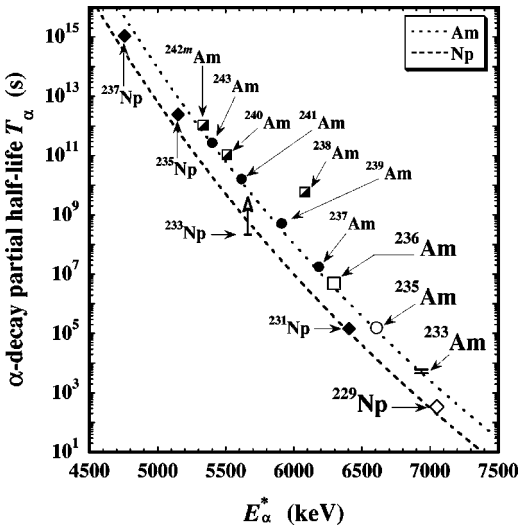

FIG. 14. α-decay partial half-lives for odd-A $^{233-243}$Am and $^{229-237}$Np, and even-A $^{236-242m}$Am plotted as a function of the α-transition energy. Two curves of Am (dotted line) and Np (dashed line) are drawn using semiempirical constants $A(Z)$ and $B(Z)$ interpolated from the adjacent even elements. The closed circle, half-closed square, and diamond denote α transitions for odd-A of $^{237-243}$Am, even-A of $^{238-242m}$Am, and odd-A of $^{231-237}$Np, respectively. The open circle, square, and diamond indicate the partial half-lives observed in this work for odd-A ^{233}Am, even-A ^{236}Am, and odd-A ^{229}Np, respectively. The value of ^{233}Am is plotted up to the lower limit of α-decay partial half-life with the hindrance factor $F=1$ (see text).

$$\log_{10} T_\alpha = A(Z)(E^*_\alpha)^{-1/2} + B(Z), \tag{4.1}$$

where $A(Z)$ and $B(Z)$ are the constants for each element that give the best fit to the data points, and Z denotes the atomic number of the α daughter nuclide. The E^*_α defined in this equation is derived from the measured α-particle energy E_α through the following equations:

$$E^*_\alpha = (A_p/A_d)E_\alpha + \Delta E_{sc} \tag{4.2}$$

and

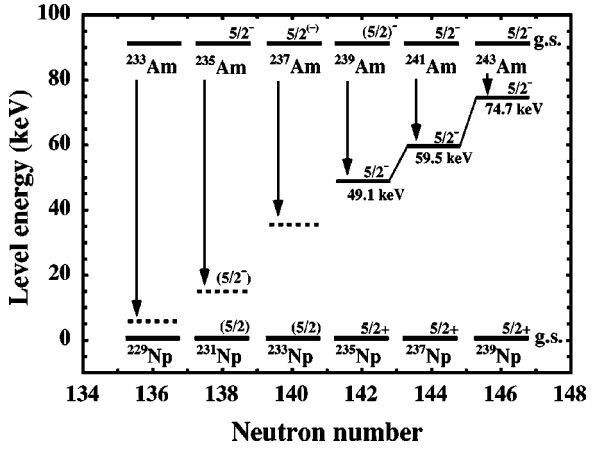

FIG. 15. Excitation energy levels of odd-A $^{229-239}$Np isotopes as a function of the neutron number. Data from Ref. [14].

TABLE II. Hindrance factor F estimated for odd-A Am and Np isotopes. g.s. stands for ground state.

Odd-A nuclide	α transition [14]	E_α^* (keV)	$_{\text{expt}}T_{1/2}^{\alpha}$ (s)	$_{\text{favored}}T_{1/2}^{\alpha}$ (s)	F
^{233}Am		6937	<6400	4700	<1.4
^{235}Am		6607	1.55×10^{5}	1.25×10^{5}	1.2
^{237}Am	$(5/2^-)$ for g.s. $^{237}\text{Am}\rightarrow{}^{233}\text{Np}(5/2^-)$	6184	1.76×10^{7}	1.23×10^{7}	1.4
^{239}Am	$5/2^-[523]\rightarrow{}^{235}\text{Np}\ 5/2^-[523]$	5911	5.12×10^{8}	3.07×10^{8}	1.7
^{241}Am	$5/2^-[523]\rightarrow{}^{237}\text{Np}\ 5/2^-[523]$	5616	1.60×10^{10}	1.29×10^{10}	1.2
^{243}Am	$5/2^-[523]\rightarrow{}^{239}\text{Np}\ 5/2^-[523]$	5402	2.66×10^{11}	2.35×10^{11}	1.1
^{229}Np		7049	343	196	1.8
^{231}Np	(5/2) for g.s. $^{231}\text{Np}\rightarrow{}^{227}\text{Pa}(5/2)$	6405	1.46×10^{5}	1.11×10^{5}	1.3
^{233}Np	$(5/2^+)$ for g.s. $^{233}\text{Np}\rightarrow{}^{229}\text{Pa}(5/2^+)$	5664	$>2.17\times10^{8}$	5.95×10^{8}	>0.36
^{235}Np	$5/2^+[642]\rightarrow{}^{231}\text{Pa}\ 5/2^+[642]$	5149	2.48×10^{12}	6.75×10^{11}	3.7
^{237}Np	$5/2^+[642]\rightarrow{}^{233}\text{Pa}\ 5/2^+[642]$	4756	1.09×10^{15}	3.07×10^{14}	3.6

$$\Delta E_{sc} = (6.5\times10^{-2})Z^{7/5}\ \text{keV}, \tag{4.3}$$

where A_p and A_d refer to the mass number of the parent and daughter nuclides, respectively, and ΔE_{sc} is the correction factor for the electron screening [21]. In Figs. 13(a) and 13(b) are plotted those constants obtained for the α-emitting parents of even-even nuclides of each element for $(Z+2)=92-98$. To evaluate the hindrance factors of the odd-A ^{233,235}Am and ^{229}Np and even-A ^{234,236}Am nuclides, the values of the constants $A(Z)$ and $B(Z)$ for Am and Np were deduced by interpolation from the neighboring elements. As a result, $A(Z)$ and $B(Z)$ for Am are valued at 152.23 (keV) and −54.13 (keV), while those for Np are 148.9 (keV) and −53.79 (keV), respectively. Figure 14 shows two curves drawn for the expected, favored transitions for Am and Np and the reference data for $^{237-242m}$Am and $^{231-237}$Np, together with the data obtained in the present work for ^{236}Am, ^{235}Am, ^{229}Np, and ^{233}Am. The deviations of the experimental α-decay partial half-lives from the corresponding Am and Np curves at the same E_α are defined here as hindrance factors F, and they are expressed as ratios. Tables II and III show the experimental and expected α-decay partial half-lives for favored transitions, α-transition energies, hindrance factors F, and the assigned Nilsson levels involved in the α transitions, if known, for odd-A $^{233-243}$Am and $^{229-237}$Np, and for even-A $^{234-242m}$Am, respectively. It is found that the hindrance factors for odd-A ^{235}Am and ^{229}Np and for even-A ^{236}Am measured in this work are close to 1.

Since the results of the γ-γ coincidence measurements for ^{235}Am revealed that the ground state of ^{235}Am has the $\pi5/2^-[523]$ configuration [11], the energy level in the daughter ^{231}Np fed by the α-decay is expected to be the $\pi5/2^-[523]$ configuration from the evaluated F value. This assignment of the transition for ^{235}Am is the same with the well-established favored transition from the ^{241}Am $\pi5/2^-[523]$ to the $\pi5/2^-[523]$ level of ^{237}Np. As neutron-deficient actinides with $A\geqslant225$ are commonly deformed to $\epsilon_2=0.2-0.3$ as estimated in Ref. [22], it is expected from the Nilsson diagram that the 93rd proton would occupy one of the two configurations $\pi5/2^-[523]$ or $\pi5/2^+[642]$ as the ground state. For examining the systematic features of the energy levels of those states, we depict the energy levels of the $\pi5/2^-[523]$ state and the ground state configurations of the neighboring odd-A Np isotopes (^{235}Np, ^{237}Np, and ^{239}Np) as shown in Fig. 15. All of the odd-A Np nuclides $^{235-239}$Np have the $\pi5/2^+[642]$ configuration in the ground state bandhead, and the $\pi5/2^-[523]$ state lies very close to the $\pi5/2^+[642]$ state, whose energy difference becomes smaller with decreasing neutron number. This tendency can explain the absence of detected α-γ coincidence events in the α-decay of ^{235}Am, as described in Sec. III B. During the course of the configuration assignment in odd-A Am α transitions, the observed lower branching limit and the F value close to unity for the α transition of ^{233}Am also suggest that this transition is between the ^{233}Am $\pi5/2^-[523]$ and the ^{229}Np $\pi5/2^-[523]$. In addition, the observed α-decay of ^{233}Am with the upper limit of the hin-

TABLE III. Hindrance factor F estimated for even-A Am isotopes.

Even-A nuclide	α transition [14]	E_α^* (keV)	$_{\text{expt}}T_{1/2}^{\alpha}$ (s)	$_{\text{favored}}T_{1/2}^{\alpha}$ (s)	F
$^{236}\text{Am}^{g+m}$	$\pi5/2^-[523]\nu5/2^+[633]$ for g.s. ^{236}Am	6294	4.95×10^{6}	3.57×10^{6}	1.4
^{238}Am	$\pi5/2^-[523]\nu7/2^-[743]\rightarrow{}^{234}\text{Np}(0^+)$	6080	5.88×10^{9}	4.09×10^{7}	143.9
^{240}Am	$\pi5/2^-[523]\nu1/2^+[631]\rightarrow{}^{236}\text{Np}\ \pi5/2^-[523]\nu1/2^+[631]$	5507	1.11×10^{11}	5.54×10^{10}	2.0
$^{242}\text{Am}^{m}$	$\pi5/2^-[523]\nu5/2^+[622]\rightarrow{}^{238}\text{Np}\ \pi5/2^-[523]\nu5/2^+[622]$	5333	1.08×10^{12}	6.22×10^{11}	1.7

TABLE IV. Experimental Q_α(expt) values are compared with the evaluated and theoretical ones. The symbol Δ means a deviation between the Q_α(expt) values and the evaluated and theoretical ones.

Nuclide	Q_α(expt)[a] (keV)	Audi and Wapstra [26] (keV)	Möller *et al.* [27] (keV)	Koura *et al.* [28] (keV)
^{233}Am	6898±17	7100±235	7110	7459
Δ		202	212	561
^{235}Am	6569±14	6700±212	6600	7237
Δ		131	31	668
^{236}Am	6286±40	6397±141	6470	7105
Δ		111	184	819

[a]The observed α transitions are assumed to be ground-to-ground state transitions.

drance factor $F=1.4$ suggests that the F value for ^{233}Am is in the range of 1.0–1.4. Thus, the α branching I_α should be constrained to lie between 3.0×10^{-2} and 5.0×10^{-2} as plotted by a bar symbol in Fig. 14.

For the α-decays of odd-A $^{229-237}$Np shown in Table II, all the hindrance factors except for ^{233}Np are within the range of 1–4. The α branching I_α of ^{233}Np is merely evaluated as an upper limit value in Refs. [23,24], and the hindrance factor is deduced to be >0.36. It is reasonable to suppose from such small hindrance factors that these α transitions are regarded as the favored transitions, although the hindrance seems to be a little larger for the heavier isotopes of Np than for the lighter ones.

For α-decays of even-A ^{234}Am, we suggest that the 6.46 MeV α group of ^{234}Am reported in Ref. [1] must be assigned to the α-decay of ^{235}Am. Hall *et al.* [1] concluded that the α-decay of ^{235}Am could be ignored in their experiment when the predicted cross sections for the ^{237}Np(^{4}He, xn)$^{241-x}$Am reactions were considered. However, we have estimated that the appearance of α-decay events from ^{235}Am is probable and cannot be excluded. Since no mass separation was performed in Ref. [1], they could not definitely determine where the α-particle group of 6.46 MeV came from, ^{234}Am or ^{235}Am. If the α-decay curve is analyzed with one component in the Hall's half-life analysis instead of two components as they assumed, the calculated half-life turns out to be about 9 min, which is in good agreement with the 10.3±0.6 min half-life of ^{235}Am determined in the present study. For these reasons, it is reasonable to point out that the 6.46 MeV α group in Ref. [1] could have originated from the α-decay of ^{235}Am. However, in the present paper we simply state that the upper limit of the α-branching intensity of ^{234}Am for the 6.46 MeV α group is $I_\alpha<4.0\times10^{-4}$. In Table III are summarized the hindrance factor F of ^{236}Am together with those of the heavier even-A Am. It is revealed that the F value of ^{236}Am is almost equal to those of other even-A ^{240}Am and ^{242}Am^m, except for ^{238}Am (a hindrance factor value of 110 for ^{238}Am is reported by Ahmad *et al.* [25], who calculated it from the spin independent theory of Preston [20] and concluded that its transition was not a favored transition) and is also in the range of $F=1.1-1.7$ observed for the α transitions of odd-A ^{239,241,243}Am nuclei regarded as the favored transitions (see Table II). Therefore, it is made clear that the observed α-decay of ^{236}Am in the present work can be regarded as a favored transition.

In Table IV are presented Q_α(expt) values obtained from the present results of α-particle energies E_α of ^{233,235,236}Am with an assumption of the ground-to-ground transition, together with the evaluated values from the mass table by Audi and Wapstra [26] and theoretical values based on the finite-range droplet model (FRDM) by Möller *et al.* [27] and on the Koura-Uno-Tachibana-Yamada (KUTY) formula by Koura *et al.* [28]. Although the predicted values are systematically larger than the experimental ones for ^{233,235,236}Am, the semiempirical values by Audi and Wapstra and the theoretical one by Möller *et al.* can well account for the experimental values in the range below ~200 keV.

V. CONCLUSION

We have observed the α transition of ^{235}Am for the first time. The α-particle energies of ^{233}Am and ^{235}Am were determined to be 6780±17 keV and 6457±14 keV, and their half-lives were measured to be 3.2±0.8 min and 10.3±0.6 min, respectively. The α branchings I_α of ^{235}Am and of ^{229}Np, the α-decay daughter of ^{233}Am, were determined to be $(4.0\pm0.5)\times10^{-3}$ and 0.68±0.11, respectively, and the lower limit of α branching for ^{233}Am was deduced to be 3×10^{-2}. Using a well-known systematic formula relating α-particle half-life $T^\alpha_{1/2}$ and α-transition energy E^*_α, we have evaluated the hindrance factors for odd-A Am and Np and for even-A Am. It was found that those observed α transitions of ^{233}Am, ^{235}Am, ^{236}Am, and ^{229}Np had hindrance factors close to unity, and thus, they could be regarded as the favored transitions. In addition, we have obtained the Q_α(expt) values of ^{233,235,236}Am derived from their measured α-particle energies.

ACKNOWLEDGMENTS

The authors wish to thank the staff and crew of the JAERI tandem accelerator for providing the intense and stable ^{6}Li beam. This work was partly carried out by Universities-JAERI Joint Research Project on the Back-End Chemistry of the Nuclear Fuel Cycle.

[1] H. L. Hall *et al.*, Phys. Rev. C **41**, 618 (1990).
[2] H. L. Hall *et al.*, Phys. Rev. C **42**, 1480 (1990).
[3] H. L. Hall, Ph.D thesis, Lawrence Berkeley Laboratory, LBL-27878, 1989.
[4] J. Guo *et al.*, Z. Phys. A **355**, 111 (1996).
[5] K. Tsukada *et al.*, Phys. Rev. C **57**, 2057 (1998).
[6] M. Sakama *et al.*, Eur. Phys. J. A **9**, 303 (2000).
[7] S. Ichikawa, K. Tsukada, M. Asai, H. Haba, M. Sakama, Y. Kojima, M. Shibata, Y. Nagame, Y. Oura, and K. Kawade, Nucl. Instrum. Methods Phys. Res. B **187**, 548 (2002).
[8] Y. Hatsukawa, N. Shinohara, K. Hata, K. Tsukada, Y. Oura, S. Ichikawa, I. Nishinaka, Y. Nagame, and M. Oshima, JAERI Review **96–011**, 42 (1996).
[9] K. Yamamoto, Y. Fujii, Y. Kotooka, and T. Katayama, Nucl. Instrum. Methods Phys. Res. A **253**, 542 (1987).
[10] T. Motobayashi, M. Louvel, S. M. Lee, and S. Jeong, Nucl. Instrum. Methods Phys. Res. A **284**, 526 (1989).
[11] M. Asai *et al.*, J. Nucl. Radiochem. Sci. **3**, 187 (2002).
[12] M. Sakama *et al.*, JAERI-Review **99–028**, 20 (1999).
[13] T. D. Thomas, R. Vandenbosch, R. A. Glass, and G. T. Seaborg, Phys. Rev. **106**, 1228 (1957).
[14] *Table of Isotopes*, 8th ed., edited by R. B. Firestone and V. S. Shirley (Wiley, New York, 1996).
[15] R. L. Hahn, M. F. Roche, and K. S. Toth, Nucl. Phys. **A113**, 206 (1968).
[16] R. Taagepera and M. Nurmia, Ann. Acad. Sci. Fenn., Ser. A **VI**, 78(1961).
[17] V. E. Viola, Jr. and G. T. Seaborg, J. Inorg. Nucl. Chem. **28**, 741 (1966).
[18] B. Buck, A. C. Merchant, and S. M. Perez, J. Phys. G **17**, 1223 (1991).
[19] Y. Hatsukawa, H. Nakahara, and D. C. Hoffmann, Phys. Rev. C **42**, 674 (1990).
[20] M. A. Preston, Phys. Rev. **71**, 865 (1947).
[21] J. O. Rasmussen, *Alpha-, Beta- and Gamma-ray Spectroscopy*, edited by K. Siegbahn (North-Holland, Amsterdam, 1965), p. 701.
[22] P. Möller, J. R. Nix, W. D. Myers, and W. J. Swiatecki, At. Data Nucl. Data Tables **59**, 185 (1995).
[23] L. B. Magnusson, S. G. Thompson, and G. T. Seaborg, Phys. Rev. **78**, 363 (1950).
[24] R. Weiss-reuter, H. Münzel, and G. Pfennig, J. Inorg. Nucl. Chem. **35**, 2145 (1973).
[25] I. Ahmad, R. K. Sjoblom, R. F. Barnes, J. F. Wagner, and P. R. Fields, Nucl. Phys. **A186**, 620 (1972).
[26] G. Audi and A. Wapstra, Nucl. Phys. **A595**, 409 (1995).
[27] P. Möller, J. R. Nix, and K. L. Kratz, At. Data Nucl. Data Tables **66**, 131 (1997).
[28] H. Koura, M. Uno, T. Tachibana, and M. Yamada, Nucl. Phys. **A674**, 47 (2000).